Distribution of this document is unlimited.

A NOTE ON THE DOSIMETRIC INTERPRETATION OF RIGIDITY SPECTRA FOR SOLAR PARTICLE BEAMS

Hermann J. Schaefer

Bureau of Medicine and Surgery
MFO 22.03.02-5001.34

NASA Order No. R-75

Approved by

Captain Ashton Graybiel, MC, USN
Director of Research

Released by

Captain H. C. Hunley, MC, USN
Commanding Officer

26 April 1966

U.S. NAVAL AEROSPACE MEDICAL INSTITUTE
U.S. NAVAL AVIATION MEDICAL CENTER
PENSACOLA, FLORIDA

SUMMARY PAGE

THE PROBLEM

Exposure conditions in solar particle beams in systems of very low shielding (LEM, EVA) are complicated by the fact that the nuclear components heavier than protons can contribute substantially to the total dose. Since the maximum of Solar Cycle 19 occurred several years in the past, measurements of flare produced particle fluxes by various research groups have been thoroughly compared, and the body of available information on flare spectra seems complete. Therefore, the time appears right to investigate the depth dose distribution in a human target behind very low shielding in a synoptic way, attempting to define the maximum and minimum type transition curves that might be encountered in flare events of the future.

FINDINGS

By adopting the exponential rigidity concept in the mathematical presentation of experimental data on fluxes of flare produced particle beams as proposed by Freier and Webber, three fictitious flare spectra are "synthesized" which cover the full variability range of all flux/rigidity gradients reported for flares of Cycle 19. After establishing the differential range spectra for the proton, alpha, and medium heavy components for the three theoretical spectra, the corresponding rad and rem depth dose rate distributions are evaluated. The results indicate that the relative contribution of the alpha component to the total dose strongly depends on the slope of the rigidity spectrum ranging from 40 per cent of the proton dose in the body surface for a very steep spectrum to 400 per cent for a flat spectrum. Contrary to the alpha component, the medium heavy (C, N, O) group never contributes significantly to the total exposure.

Converting rad doses to RBE dose equivalents on the basis of the RBE/LET relationship proposed by the RBE Committee of the ICRP leads to a further substantial magnification of the alpha contribution, but fails to lift the dose level of the medium heavy nuclei to more than 18 per cent of total exposure. The local RBE factors for the alpha and medium heavy components show a strong transition in near surface regions of the body, dropping to smaller values with increasing depth.

Analysis of the local range spectra in the body surface below low shielding for the steepest rigidity spectrum shows that the bulk of the alpha flux is made up of particles in the zero to 0.2 g/cm^2 range interval. Design of dosimetric instrumentation that would measure accurately the local dose for such narrow range spectra seems difficult. Still more problematic is the radiobiological interpretation of such steeply changing dose distributions in the human body in terms of radiation injury and permissible exposure.

INTRODUCTION

In assessing the true total body radiation load from exposures to solar particle beams in space, considerable difficulties arise from the ever-changing depth dose patterns. These changes reflect the great variability of the configuration of the energy spectra not only for different flare events, but even for the same event in the time course of development and decay. Particularly intricate are the exposure conditions in near surface regions of a human target in systems with a very low shielding equivalent, such as the Lunar Excursion Module (LEM) or in Extra Vehicular Activity (EVA). Under these circumstances, particles of low penetration are so rapidly removed in near surface regions of the body that the steep drop of the rad dose is accompanied by an equally steep drop of the local RBE and QF, creating exposure conditions for which no counterpart could be found in conventional radiobiology or radiotherapy.

The situation in systems of low shielding is further complicated by the fact that solar particle beams contain alpha particles in addition to protons, and, in smaller fractions, heavier nuclei. Depending on spectral configuration, the alpha component in particular can contribute substantially, or even predominantly, to the dose in near surface regions of a human target.

For the radiologist and health physicist interested in the radiation safety aspects of the peculiar type of radiation exposure in question, great difficulties in assessing the dosages involved arise from the fact that the flux/energy or flux/rigidity plots, with which the cosmic ray physicist usually describes the results of his measurements, do not lend themselves to an easy conversion to depth dose distributions which those fluxes would produce in the human body. Establishing these distributions requires rather involved computational methods. Though such analyses have been carried out repeatedly for typical flare spectra (1-4), it seems desirable to identify, in a synoptic evaluation of all large flare events of the past solar maximum, the full range of variability of rad and rem depth dose gradients that can be expected to occur in the astronaut's body in systems of low shielding. Since more than half a solar cycle has elapsed since the last solar maximum, the flare measurements of the various solar particle events of Cycle 19 as reported by different experimenters by now have been thoroughly discussed and compared and found in essential agreement. The time therefore seems right for a general analysis of the indicated kind. The following study is an attempt in this direction. Based on the spectra of the six largest flare events of Cycle 19, three "synthetic" flare spectra have been constructed that cover the full variability of all physical parameters of the six real events, yet demonstrate more systematically the corresponding changes in the basic dosimetric quantities.

RIGIDITY AND RANGE SPECTRA FOR TYPICAL FLARE EVENTS

For the graphical presentation of flux measurements of solar particle beams, experimenters have used both the flux/energy (5) and the flux/rigidity (6) plot. For a computational analysis of depth dose distributions, both methods require lengthy conversion procedures since neither energy nor rigidity of different nuclear particles

is in a simple and direct way related to penetrating power. Freier and Webber (l.c., 6) have shown that the analytical formulation of flux measurements is especially concise if rigidity is used as both independent variable and constant parameter. By this approach, the ever-changing spectral configuration of flare beams can be described with the same mathematical expression containing only two parameters, a flux and a rigidity constant, that vary for different spectra. Unfortunately, as just mentioned, the corresponding depth dose patterns cannot be established from the rigidity spectra by an equally simple method. For instance, in the rigidity interval of interest for systems of low shielding, a proton, an alpha particle, and a C nucleus of the same rigidity have relative penetrating powers of 100:40:1. This shows that plotting the fluxes of different nuclear particles of a flare beam over the same rigidity scale cannot convey information on relative penetrating powers nor allow inferences on depth dose distributions. For the latter purposes the range spectrum is a much more descriptive way of presenting flux data. Converting rigidity spectra to range spectra is a routine procedure. Applied to identical rigidity spectra for different nuclei, such as protons, alpha particles, and C nuclei, it leads to greatly different range spectra for each component as will be shown presently.

The rigidity spectra for the six largest solar particle events of the past cycle as compiled by Freier and Webber (l.c., 6) are shown in the left-hand graph of Figure 1.

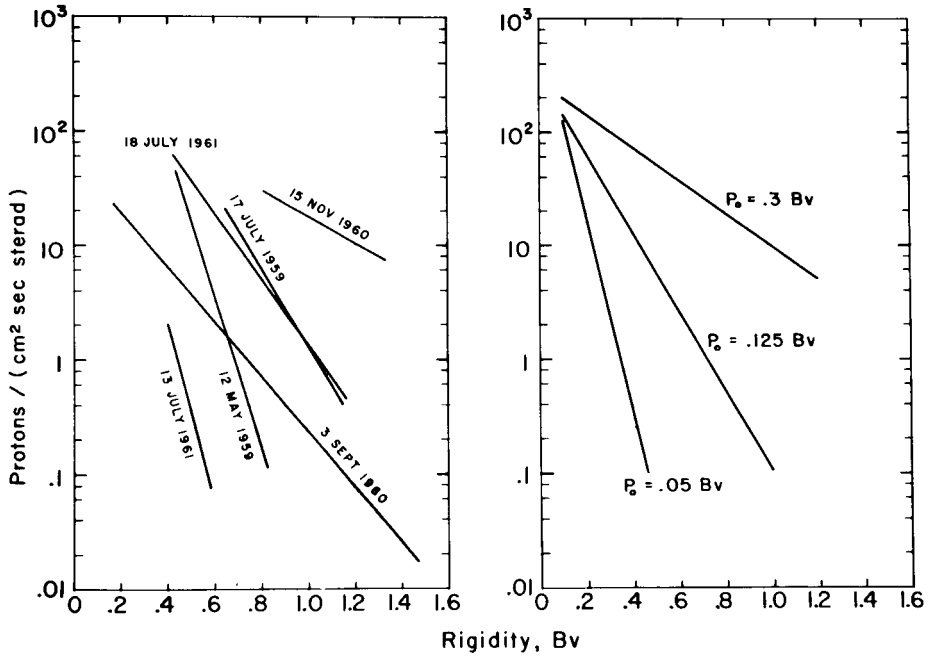

Figure 1

Rigidity Spectra of Solar Particle Beams

Left: Spectra of six large flare events of the past solar cycle.

Right: Model spectra used for analysis. The three fictitious spectra have been designed to cover the full flux/rigidity area and slope variability of any possible flare event. Spectra are normalized to furnish equal proton dose rates in tissue surface behind 0.1 g/cm^2 shielding (see Figure 3).

They demonstrate well the really enormous variations in absolute flux values and flux/rigidity gradients between different flares, yet all six spectra obey the exponential law $J = J_o \exp(-P/P_o)$ where J_o and P_o are a flux and a rigidity constant different for each event. The J_o and P_o values for the six spectra are tabulated in Table I.

Table I

Constants of Six Flare Spectra of Solar Cycle 19 Shown in the Left Graph of Figure 1

Date of Flare	J_o*	P_o*
10 May 1959	30,000	65
16 July 1959	3,200	125
3 September 1960	60	180
15 November 1960	250	375
12 July 1961	850	60
18 July 1961	1,000	150

*J_o is given in Protons/(cm^2 sec sterad), P_o in Mv.

At this point, it should be mentioned that each spectrum of Figure 1 describes the spectral configuration only as it prevailed during a certain limited time span of the flare event. The spectral evolution as it occurred during development and decay of the flare produced radiation surge is not taken into consideration. However, as can be seen from the original reference (l.c., 6) the six spectra as a whole cover very well also the variations that the individual event would show during its development and decay. In other words, the six spectra delineate the boundaries in the flux/rigidity plane within which the spectrum of any flare event can be expected to be confined. Specifically, the flux/rigidity gradient, i.e., the slope of the spectrum, of the July 13, 1961 flare can be considered as the maximum and that of November 15, 1960 flare as the minimum gradient ever to occur. Accordingly, three fictitious spectra shown in the right-hand graph of Figure 1 have been constructed showing the just-mentioned two extreme and one intermediate gradients. At the same time, the flux constants J_o of these three spectral models have been adjusted in such a way that the dose rate from the proton component in the surface of a tissue target behind 0.1 g/cm^2 shielding is equal to 1.0 rad/hour for all three spectra.

As mentioned before, the terms, $\exp(-P/P_o)$, are identical for all nuclear components of a flare event. This circumstance is the specific reason for the preference

cosmic ray physicists give to the rigidity concept for presenting flare data. Merely the flux constants J_o differ, in the individual event, for different nuclear components. It is customary to denote the relative abundances of alpha and medium heavy (C, N, O) nuclei in solar particle beams by the proton/alpha and alpha/MH ratio. In this notation, a low ratio means a high relative abundance of the heavier component. Proton/alpha ratios as low as 1.0 have been measured repeatedly. Only a few alpha/MH ratios have been reported so far, indicating an approximate value of 60. Since in the present context the maximum possible contributions of the nuclear components heavier than protons to the total dose are of interest, the computational analysis has been carried out for a proton/alpha/(C, N, O) rigidity flux ratio of 60:60:1.

The J_o and P_o constants for the three model spectra are tabulated in Table II. It should be noted that the J_o values listed hold for the proton flux. For the indicated flux ratio of 60:60:1, the alpha component would show the same flux as the proton component, and the C, N, O component would show 1/60 of that flux. The total rigidity flux constant for the entire beam, comprising all nuclear components, then, would be 2.0167 J_o. Since tissue dosages at any depth depend in a strictly linear way on J_o, the data in this report can be easily used to establish close estimates of dosages for flare spectra with any other pairs of J_o, P_o parameters by interpolation. The normalization of all data to a proton dose rate in the tissue surface of 1.0 rads/hour has been carried out specifically for facilitating such estimates.

Table II

Constants of Three Model Spectra Shown in Right-Hand Graph of Figure 1*

P_o	J_o	J_{100}
50	991	134
125	316	142
300	275	197

*For units, consult Table I. J_{100} denotes flux at 100 Mv, i.e., at the left end of spectrum in graph.

Since the C, N, O component, as will be seen later, contributes only insignificantly to the total exposure at all levels and for all P_o values, the element carbon (C) has been selected as group representative, and the LET/energy and range/energy relationships for C have been substituted for the entire group in the interest of reducing the computational workload. This simplification seems all the more acceptable in view

of the small differences in the Atomic Numbers 6, 7, and 8 of the element C, N, and O.

Figure 2 shows the differential range spectra for the three rigidity spectra in the right-hand graph of Figure 1. Since each rigidity spectrum splits up into three different range spectra for the three nuclear components, a total of nine range spectra is obtained. In the context of the present investigation where interest centers on the depth dose distribution, the flux/range gradient is of special concern. It is seen that, quite generally, this gradient decreases as P_o increases. Of special significance is the fact that the flux/range gradient of the proton component is substantially smaller than the corresponding gradients for the alpha and C components at all P_o values. This indicates that the depth of penetration of protons is substantially larger than that of alpha particles and C nuclei. It is also interesting to note that between the latter two components, there is very little difference in this respect. A third characteristic is the marked increase of the relative fluxes of the two heavier components as compared to protons for increasing P_o. Since the energy dissipation per particle, i.e, the LET, also is larger for the heavier nuclear species, the larger relative fluxes of the heavier components for larger P_o values can be expected to appear further magnified in the tissue dosages.

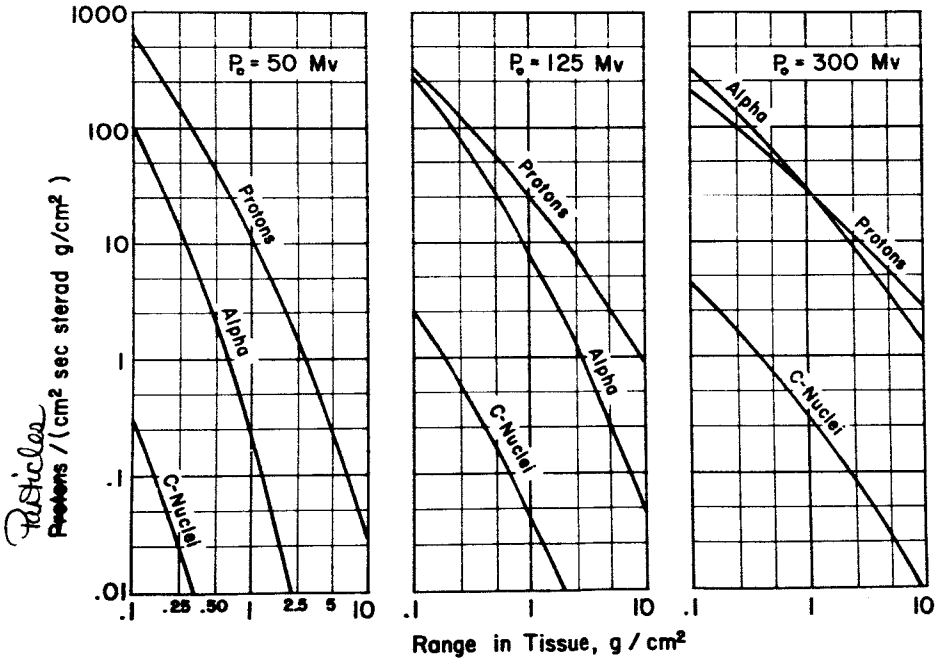

Figure 2

Differential Range Spectra of Fictitious Representative Solar Particle Beams

Spectra correspond to three rigidity spectra at right in Figure 1. Since rigidity and range of different nuclear particles are disparate magnitudes, the same rigidity spectrum leads to a different range spectrum for a different particle.

The foregoing brief survey of the basic characteristics of the range spectra of solar particle beams demonstrates well that the range spectrum is a much more meaningful way of presenting flux data than the rigidity spectrum if the depth of penetration in compact targets behind given shield configurations is to be analyzed. To be sure, for a quantitative appraisal of the exposure within the target, it is necessary to go one step further and to evaluate the range spectra in terms of absorbed energy at different depths in the target. The results of this analysis shall be presented now.

DEPTH DOSE DISTRIBUTIONS FOR STANDARD SPECTRA

In the context of the present investigation, main interest centers on the dose distribution in near surface regions of a human target behind low shielding. For flux spectra of a more or less pronounced negative slope, i.e., for spectra with a decreasing flux for increasing particle range, the exposure in the surface regions of a larger target such as the human body is determined predominantly by the particles within a limited solid angle about the vertical on the body surface. Particles incident at oblique or grazing angles and, even more, those incident upon the opposite side of the body are attenuated to insignificant flux levels because of their long pathways in tissue and shield material. Therefore, their contributions to the exposure in near surface regions are negligibly small. This means that the exposure geometry is essentially identical with that of a semi-infinite slab behind a plane shield irradiated by a particle stream arriving from all directions of the front half-space(2π incidence).

The computational analysis of the depth dose distributions for the just-described system was carried out by numerical methods. The half-sphere of the sky as source of the incident radiation was broken down into 20 ring-shaped solid angles of equal size. Each of these elementary solid angles was represented in the integration by its mean angle of incidence and its corresponding mean absorption pathway in shield and body. The differential range spectra were broken down into intervals of 0.0025 g/cm^2 width up to the range of 3 g/cm^2 and from there on into intervals of 0.01 g/cm^2. Dosages were sampled at tissue depths in steps of 0.02 and, at greater depths, of 0.05 and 0.1 g/cm^2.

The results of the computations are presented in Figure 3 which shows the depth dose distributions for the nine range spectra of Figure 2. The reader is reminded again that the flux constants J_o of the three model spectra have been adjusted beforehand to produce the same dose of 1.0 rad/hour in the tissue surface for the proton component of all three spectra. This normalization allows a direct comparison of the dose contributions from the alpha component for the three rigidity spectra. The curves in Figure 3 demonstrate conspicuously the very strong dependence of the alpha dose on the rigidity constant P_o, i.e., on the slope of the rigidity spectrum. As P_o increases, i.e., as the slope decreases and the spectrum hardens, the alpha contribution to the surface dose changes from 40 per cent of the proton dose for P_o = 50 Mv to 400 per cent of the proton dose for P_o = 300 Mv. In other words, the alpha component becomes, for the hardest spectrum, the predominant contributor to the total dose. Despite the fact that the alpha dose has a considerably steeper depth gradient than the proton dose,

the predominance of the alpha component is maintained to tissue depths well beyond 2 g/cm^2. For the spectrum of intermediate slope (P_o = 125 Mv) the ratio of the alpha to the proton dose is smaller than for the hardest spectrum (P_o = 300 Mv), but the alpha dose is still a substantial contributor to the total exposure. It accounts, in the tissue surface, for 215 per cent of the proton dose and already becomes equal to the latter at 5 millimeter depth.

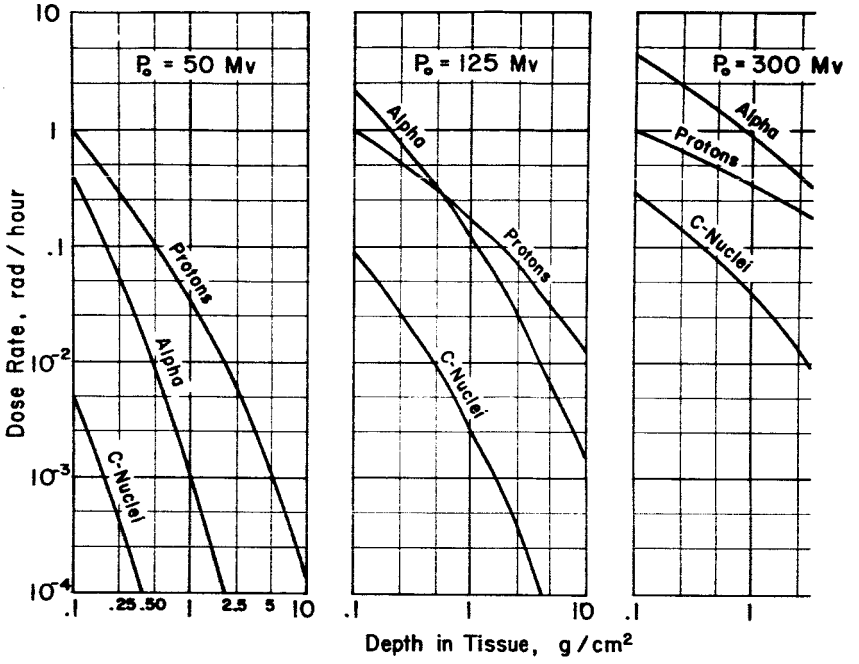

Figure 3

Depth Dose Distribution for Range Spectra of Figure 2

Note strong increase of alpha doses as P_o increases, i.e., as spectra harden.

It should be mentioned at this point that a proton/alpha rigidity flux ratio of 1.0 so far has not been actually reported for a spectrum with a P_o = 300 Mv. The highest P_o for which a ratio of 1.0 has been found is 175 Mv (l.c., 6). This, however, is not to be understood in the sense that the proton/alpha rigidity ratios for spectra with P_o values larger than 175 Mv are smaller, but it simply means that, so far, measurements of alpha fluxes on harder spectra have not been carried out. Quite generally, available information on alpha fluxes in solar particle beams is substantially smaller than on protons because of the lower penetrating power of alpha particles which, in turn, makes the so-called instrument cut-off a much more difficult problem in the experimental design. The few alpha data on flare beams presently available are by far not sufficient to allow inferences on a possible general correlation between the proton/alpha flux ratio and P_o. For the time being, therefore, the question must remain unsettled whether such extremely high relative alpha dosages as are indicated in the triplet of depth dose distributions for P_o = 300 Mv in Figure 3 could be encountered in actual flare events.

For a complete dosimetric analysis, dose rates in rad/hour have to be converted to equivalent dose rates in rem/hour, taking into consideration the LET distributions of the beam components. As pointed out in an earlier study (7), this conversion encounters principal difficulties for the alpha component and all the more for C nuclei inasmuch as official recommendations provide specific Relative Biological Effectiveness (RBE) and Quality Factor (QF) data only up to an LET value which falls considerably short of the maximum LET for the components in question. As a conservative but otherwise entirely arbitrary way out of this difficulty, an RBE/LET relationship has been adopted which follows official recommendations up to the LET of 150 kev/micron T and then gradually saturates at the constant value of 10 for the entire remainder of the LET scale. It is the same relationship that has been used in the earlier study (Figure 3 in l.c., 7). Application of this RBE/LET relationship to the local dose rates of the three nuclear components requires a rather complex computational procedure since the local LET distribution changes continuously as the radiation penetrates into the target.

In the earlier study, the results of the indicated analysis were presented in terms of the rem dose equivalents corresponding to the absorbed doses. In the context of the present investigation, in which interest centers upon the relative changes in the intra-target dose distribution for different types of incident spectra rather than on absolute dose levels as such, it is more descriptive to show the transition curves of the local RBE factors themselves since they reflect directly the changes in the LET distribution independent of the dose level. The pertinent data are presented in Figure 4. It is seen that the alpha and C components show a pronounced decrease of the local RBE extending down to tissue depths well beyond 1 g/cm^2. The steepness of this decrease is markedly greater for smaller P_o values though it does not match by far the steepness of the rigidity and range spectra.

With regard to the absolute rem dose levels, which can be easily obtained by multiplying related ordinate values of Figures 3 and 4, it is seen by inspection that the importance of the alpha component as contributor to total exposure is further substantially magnified. This is not so for the C component despite the much larger RBE factors because the rad doses of this component are extremely small and are not lifted to more than 18 per cent of the total exposure if they are converted to rem doses.

If exposure data are presented in terms of RBE dose equivalents, the radiobiologist usually assumes a reserved attitude in view of the many simplifying assumptions contained in the RBE concept. In this respect, it should not be overlooked that the transition of the local RBE as shown in Figure 4, quite aside from any problematic radiobiological meaning of particular RBE values as such, truly reflects the transition of the local LET distribution because an accurately defined RBE/LET relationship has been used for establishing the RBE/depth functions. Since, in this operation, the mean RBE substitutes for an entire LET spectrum, the complex transition of the latter is demonstrated in a much more concise manner.

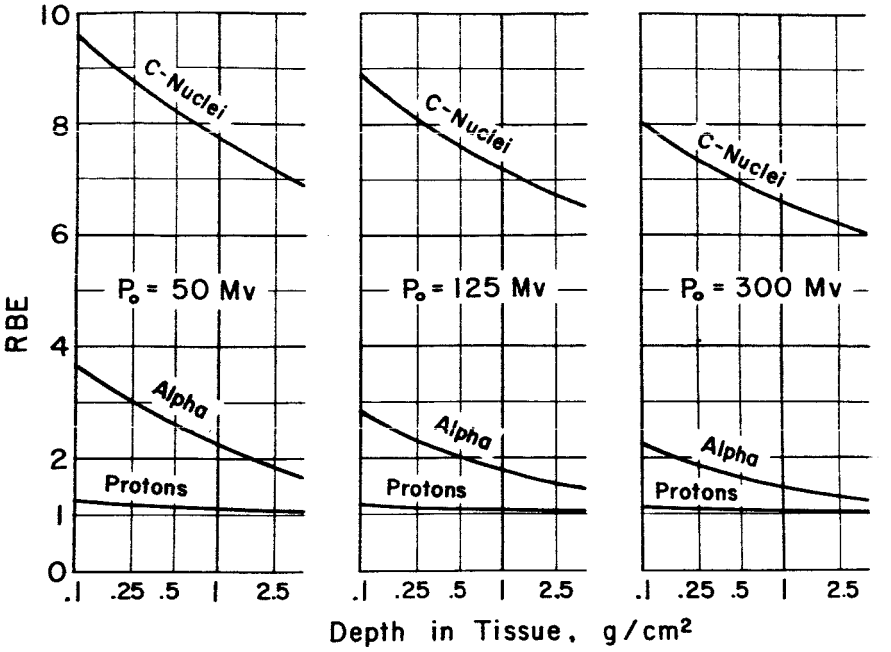

Figure 4

Local RBE in Tissue for Spectra of Figure 2

RBE has been determined according to the RBE/LET relationship recommended by the RBE Committee of the ICRP using extrapolation saturating at RBE = 10 beyond 150 kev/micron T.

DISCUSSION

The main result of the present study is that, of the components heavier than protons in solar particle beams, only alpha particles can contribute significantly to total exposure. The alpha dose fraction varies greatly from an insignificant to a predominant level depending on the proton/alpha flux ratio and the rigidity constant of the individual event. While the two just-named parameters serve well to define the alpha contribution to the total dose at all depths of the target and for all shield configurations, present knowledge of the basic mechanisms involved in particle acceleration in solar flares and their subsequent propagation in space is insufficient for establishing any general criteria for the proton/alpha flux ratios in different flare beams.

With regard to the implications for operational dosimetry on space missions, it is obvious that a separate determination of the alpha contribution in flare exposure seems desirable especially in space systems of low shielding. As demonstrated in Figure 4, RBE dose equivalents in near surface regions of the body are substantially larger than rad doses. Since, for solar particle beams, radiation levels in the skin are anyway by far the highest as compared to all other body tissues, accurate measurement of the rem dose on the body surface is indispensable if objectionable exposure levels are likely to

develop. On the other hand, the probability of an astronaut being caught unexpectedly by a large flare under conditions of very low shielding and not having the means of returning into the spacecraft with its heavier shielding equivalent, does not seem very high.

A final conclusion, from the standpoint of operational dosimetry possibly the most important one, concerns the question of required and attainable accuracy and resolution of dose determination. The point in question is demonstrated best by an example. As can be easily seen from the pertinent ordinate values in Figures 3 and 4, the rem dose at 1 millimeter tissue depth is, for the P_o = 50 Mv spectrum, only 40 per cent of its value in the tissue surface. For such a steep drop of local dose, it becomes both radiobiologically and dosimetrically quite problematic how to define and to determine the local exposure. Even if one would build a microsensor that could measure, in a tissue phantom, the depth dose in steps of a fraction of a millimeter, interpretation of the readings of the instrument in terms of the true radiation burden of the skin, i.e., of the dose in the stratum germinativum, still would be problematic.

Aside from the dosimetric problems posed by these extremely steep depth dose distributions, a more principal question concerns the error propagation in the evaluation procedure that leads from the rigidity spectrum to the depth dose distribution. The straight lines representing the rigidity spectra in Figure 1 are the lines of best fit through a number of experimentally determined points in the flux/rigidity coordinate system. The inherent limitations of accuracy in this process of curve fitting for the rigidity spectra obviously are transmitted to the range spectra. It seems of interest to investigate how these limitations are reflected in the local range spectra at a specific location in the target. For the tissue surface behind 0.1 g/cm^2 shielding, the local range spectra for the proton and alpha components are shown in Figure 5. In order to allow a direct comparison of beams with different P_o, fluxes have been normalized and are expressed in percentage of total local flux. Singling out the alpha curve for P_o = 50 Mv in the lower graph of Figure 5, one sees that about 85 per cent of the local alpha flux in the tissue surface consists of particles of 0.2 g/cm^2 range or less with the residual 15 per cent still heavily centering on low ranges. In other words, at the particular location chosen, the bulk of the local flux is made up of particles of very low range. In the evaluation procedure, this flux in the narrow range interval is derived from a spectrum that is based on experimental points more or less far apart from the location of the critical interval on the range scale. It should be obvious that a determination of dose from a flux obtained in the indicated indirect way from the slope of a rigidity spectrum could not be relied upon for actual operational dosimetry. In the present context, it is acceptable since it is used for analyzing the basic functional relationship involved in order to define the maximum and minimum type depth dose distributions that might occur in different flare events.

It has been suggested to carry out operational dosimetry during flare exposure by spectrometric analysis of the incident radiation and to establish the absorbed doses in the bodies of the crew from the known shield distribution of the spacecraft essentially in the same way this has been done in the present investigation. The pitfalls of such a

procedure should be quite obvious from the data in Figure 5. It does not seem an overly cautious estimate that errors in skin dose assessment exceeding 100 per cent might easily occur in such a procedure. Under exposure conditions in solar particle beams, where the integral dose that will have accrued until the event is over might well reach levels of acute radiation injury, such an error is absolutely unacceptable.

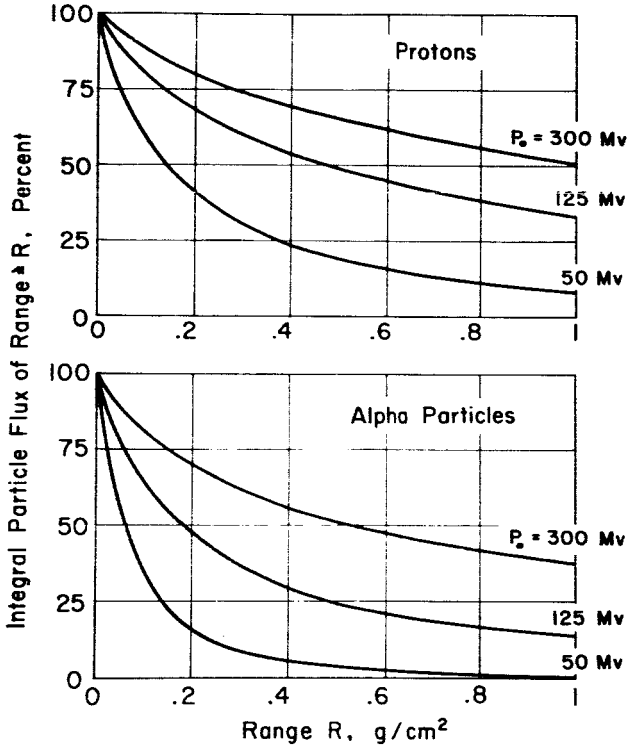

Figure 5

Local Range Spectra in Tissue Surface Behind 0.1 g/cm^2 Shielding for Spectra of Figure 2

It is seen, then, that, at least for systems of low shielding, on-the-spot measurement of dose on representative locations of the astronaut's body is the only method to obtain true information on his exposure. Rigidity spectra of the incident beam and all the more their corresponding range spectra are quite interesting and useful for studying the basic configuration of the dose distribution within the human body and for determining the requirements for operational dosimetry. In actual flight of a manned spacecraft through a solar particle beam, however, rad and rem doses at representative locations of the astronaut's body have to be measured directly.

REFERENCES

1. Schaefer, H. J., Time profile of tissue ionization dosages for Bailey's synthetic spectrum of a typical solar flare event. NSAM-810. Pensacola, Fla.: Naval School of Aviation Medicine, 1962.

2. Freier, P., and Webber, W. R., Radiation hazard in space from solar particles. Science, 142:1587-1592, 1963.

3. Dye, D. L., and Wilkinson, M., Radiation hazards in space. Science, 147: 19-25, 1965.

4. Webber, W. R., An evaluation of the radiation hazard due to solar particle events. D2-90469. Seattle, Wash.: The Boeing Company, 1963.

5. Fichtel, C. E., Charge composition of energetic solar particles. In: Hess, W. N. (Ed.), AAS-NASA Symposium on the Physics of Solar Flares. NASA SP-50. Washington, D. C.: National Aeronautics and Space Administration, 1964. Pp 263-271.

6. Freier, P. S., and Webber, W. R., Exponential rigidity spectrums for solar-flare cosmic rays. J. Geophys. Res., 68:1605-1629, 1963.

7. Schaefer, H. J., Radiation exposure from heavy nuclei in solar particle beams in space systems of low shielding. Aerospace Med., 37:1-4, 1966.

Security Classification

UNCLASSIFIED **DOCUMENT CONTROL DATA - R&D**

(Security classification of title, body of abstract and indexing annotation must be entered when the overall report is classified)

1. ORIGINATING ACTIVITY (Corporate author)	2a. REPORT SECURITY CLASSIFICATION
U.S. Naval Aerospace Medical Institute Pensacola, Florida	Unclassified
	2b. GROUP

3. REPORT TITLE A NOTE ON THE DOSIMETRIC INTERPRETATION OF RIGIDITY SPECTRA FOR SOLAR PARTICLE BEAMS

4. DESCRIPTIVE NOTES (Type of report and inclusive dates)

5. AUTHOR(S) (Last name, first name, initial)
Schaefer, Hermann J.

6. REPORT DATE	7a. TOTAL NO. OF PAGES	7b. NO. OF REFS
26 April 1966	13	7

8a. CONTRACT OR GRANT NO. NASA R-75	9a. ORIGINATOR'S REPORT NUMBER(S)
b. PROJECT NO. MFO 22.03.02-5001	NAMI-960
c.	9b. OTHER REPORT NO(S) (Any other numbers that may be assigned this report)
d.	34

10. AVAILABILITY/LIMITATION NOTICES
Qualified requesters may obtain copies of this report from DDC. Available, for sale to the public, from the Clearinghouse for Federal Scientific and Technical Information, Springfield, Virginia 22151.

11. SUPPLEMENTARY NOTES	12. SPONSORING MILITARY ACTIVITY

13. ABSTRACT

By using the experimental rigidity formulation as proposed by Freier and Webber, the particle fluxes of all flare events of the past solar cycle can be uniformly described in terms of a flux constant J_o and a rigidity constant P_o. On the basis of these data, three fictitious rigidity spectra are "synthesized" covering the full variability range of all flare events, yet characterizing more systematically the relationships between the basic dosimetric quantities and the rigidity constant P_o. It is found that, of the components heavier than protons, only alpha particles contribute substantially to total exposure. The fractional alpha dose in the tissue surface behind 0.1 g/cm^2 shielding grows from 40 per cent for P_o = 50 Mv to 400 per cent for P_o = 300 Mv. At the same time, the depth dose of the alpha component shows an extremely steep drop which would require microsensors for accurate measurement. For the alpha and medium heavy components, the RBE shows a pronounced transition in near surface regions which further steepens the drop of the RBE dose equivalents as compared to the rad doses. The extremely strong and nonlinear dependence of the rad and rem dose distribution on rigidity makes the rigidity concept practically useless for any dosimetric evaluation and indicates the need for direct measurements of local rad and rem doses on the astronaut's body.

DD FORM 1 JAN 64 1473

UNCLASSIFIED

Security Classification

Security Classification

14. KEY WORDS	LINK A		LINK B		LINK C	
	ROLE	WT	ROLE	WT	ROLE	WT
Radiation hazards in space Tissue dosages from flare produced particles in space systems of low shielding Relative Biological Effectiveness of flare produced heavy nuclei						

INSTRUCTIONS

1. ORIGINATING ACTIVITY: Enter the name and address of the contractor, subcontractor, grantee, Department of Defense activity or other organization *(corporate author)* issuing the report.

2*a*. REPORT SECURITY CLASSIFICATION: Enter the overall security classification of the report. Indicate whether "Restricted Data" is included. Marking is to be in accordance with appropriate security regulations.

2*b*. GROUP: Automatic downgrading is specified in DoD Directive 5200.10 and Armed Forces Industrial Manual. Enter the group number. Also, when applicable, show that optional markings have been used for Group 3 and Group 4 as authorized.

3. REPORT TITLE: Enter the complete report title in all capital letters. Titles in all cases should be unclassified. If a meaningful title cannot be selected without classification, show title classification in all capitals in parenthesis immediately following the title.

4. DESCRIPTIVE NOTES: If appropriate, enter the type of report, e.g., interim, progress, summary, annual, or final. Give the inclusive dates when a specific reporting period is covered.

5. AUTHOR(S): Enter the name(s) of author(s) as shown on or in the report. Enter last name, first name, middle initial. If military, show rank and branch of service. The name of the principal author is an absolute minimum requirement.

6. REPORT DATE: Enter the date of the report as day, month, year, or month, year. If more than one date appears on the report, use date of publication.

7*a*. TOTAL NUMBER OF PAGES: The total page count should follow normal pagination procedures, i.e., enter the number of pages containing information.

7*b*. NUMBER OF REFERENCES: Enter the total number of references cited in the report.

8*a*. CONTRACT OR GRANT NUMBER: If appropriate, enter the applicable number of the contract or grant under which the report was written.

8*b*, 8*c*, & 8*d*. PROJECT NUMBER: Enter the appropriate military department identification, such as project number, subproject number, system numbers, task number, etc.

9*a*. ORIGINATOR'S REPORT NUMBER(S): Enter the official report number by which the document will be identified and controlled by the originating activity. This number must be unique to this report.

9*b*. OTHER REPORT NUMBER(S): If the report has been assigned any other report numbers *(either by the originator or by the sponsor)*, also enter this number(s).

10. AVAILABILITY/LIMITATION NOTICES: Enter any limitations on further dissemination of the report, other than those imposed by security classification, using standard statements such as:

(1) "Qualified requesters may obtain copies of this report from DDC."

(2) "Foreign announcement and dissemination of this report by DDC is not authorized."

(3) "U. S. Government agencies may obtain copies of this report directly from DDC. Other qualified DDC users shall request through

_____."

(4) "U. S. military agencies may obtain copies of this report directly from DDC. Other qualified users shall request through

_____."

(5) "All distribution of this report is controlled. Qualified DDC users shall request through

_____."

If the report has been furnished to the Office of Technical Services, Department of Commerce, for sale to the public, indicate this fact and enter the price, if known.

11. SUPPLEMENTARY NOTES: Use for additional explanatory notes.

12. SPONSORING MILITARY ACTIVITY: Enter the name of the departmental project office or laboratory sponsoring *(paying for)* the research and development. Include address.

13. ABSTRACT: Enter an abstract giving a brief and factual summary of the document indicative of the report, even though it may also appear elsewhere in the body of the technical report. If additional space is required, a continuation sheet shall be attached.

It is highly desirable that the abstract of classified reports be unclassified. Each paragraph of the abstract shall end with an indication of the military security classification of the information in the paragraph, represented as *(TS), (S), (C), or (U)*.

There is no limitation on the length of the abstract. However, the suggested length is from 150 to 225 words.

14. KEY WORDS: Key words are technically meaningful terms or short phrases that characterize a report and may be used as index entries for cataloging the report. Key words must be selected so that no security classification is required. Identifiers, such as equipment model designation, trade name, military project code name, geographic location, may be used as key words but will be followed by an indication of technical context. The assignment of links, roles, and weights is optional.

UNCLASSIFIED

Security Classification